Vector boson associated with jets in CMS

Qun Wang
DESY
On behalf of the CMS Collaboration
Hamburg, 18 July 2024

HELMHOLTZ RESEARCH FOR GRAND CHALLENGES

ICHEP 2024 | PRAGUE

Outline

- V+jets measurements
  - Measurement of B(W->cq)/B(W->qq') NEW (CMS-SMP-PAS-24-009)
  - Precision measurement of the Z invisible width at 13 TeV **(**PLB 842 (2023) 137563**)**
  - Multi-differential Z+jets cross sections at 13 TeV **(**PRD 108 (2023) 052004**)**
  - Azimuthal correlations in Z+jets at 13 TeV **(**EPJC 83 (2023) 722**)**
- Summary

Measurement of B(W->cq)/B(W->qq') NEW

- Measure the W boson hadronic decay branching fraction ratio:

$$R_c^W = \frac{\mathcal{B}(W \to cq)}{\mathcal{B}(W \to uq) + \mathcal{B}(W \to cq)}$$

- SM prediction: 0.5

$$R_c^W = \frac{|V_{cd}|^2 + |V_{cs}|^2 + |V_{cb}|^2}{|V_{ud}|^2 + |V_{us}|^2 + |V_{ub}|^2 + |V_{cd}|^2 + |V_{cs}|^2 + |V_{cb}|^2}$$

- PDG value: 0.49+/- 0.04
  - Measurements at LEP (ALEPH : Phys. Lett. B 465 (1999) 349; OPAL: Phys. Lett. B 490 (2000) 71-86)
- The large cross section of top quark-antiquark production at the LHC offers a sizable high-purity sample of W bosons
  - Semileptonic ttbar has one W boson decaying leptonically, providing a lepton for the trigger and another one decaying hadronically, enabling the goal measurement
- Charm tagging and its systematics are key to conduct the measurement

Measurement of B(W->cq)/B(W->qq') NEW

- Baseline selection: high-pT isolated lepton + MET + >= 4 jets (2 b-tagged)

Year	2016	2017	2018
Muon trigger	24 GeV	27 GeV	24 GeV
Electron trigger	27 GeV	32 GeV	32 GeV

Channel	$W \to \mu\nu$			$W \to e\nu$		
Year	2016	2017	2018	2016	2017	2018
Lepton p_T^l (GeV)	>30			>35		
Lepton $\|\eta^l\|$	<2.4			<2.4		
Lepton isolation I_{comb}/p_T^l	<0.15			-		
Lepton ID	Tight ID			Tight MVA		
Number of leptons	1					
Extra leptons veto	Discard tight leptons with $p_T > 20$ GeV					
p_T^{miss} (GeV)	>20					
W transverse mass (GeV)	>20					
Jet p_T^{jet} (GeV)	>25					
Jet $\|\eta^{jet}\|$	<2.4					
ΔR (jet, ℓ)	>0.4					
#Jets	≥ 4					
B-tagged jets	2 Medium WP (btagDeepFlavB)					

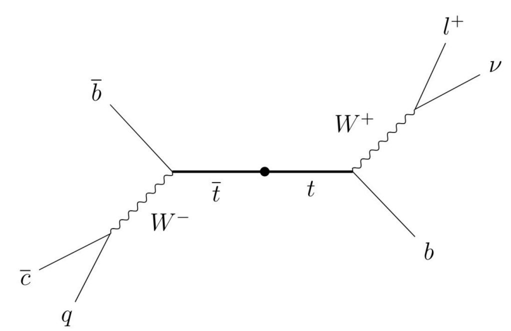

Measurement of B(W->cq)/B(W->qq') NEW

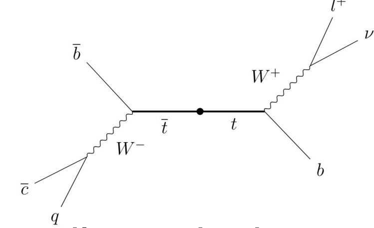

Tagging of charm jets: identification of a muon inside a jet stemming from the semileptonic decay of the charm hadron

- Muon with $\Delta R(\mu, \text{jet}) < 0.4$, excluding the two b-tagging jets
- Tight ID, non-isolation requirement: $I_{comb} > 2.5$ GeV
- Transverse momentum $\in [5,25]$ GeV, $p_T^{\mu}/p_T^{jet} < 0.5$
- Opposite-sign requirement (muon in jet and isolated lepton have opposite electric charge sign)

Calibration of the charm tagging efficiency in the simulation

- Muon production
  - Charm hadron production => charm fragmentation fractions is reweighed in MC
  - Charm hadron decay => decay branching fractions to muon+X is corrected.
- Muon reconstruction
  - Reconstruction/identification efficiency => calibration using muons in bottom jets

The background for the charm-tagged selection is determined from data using the same-sign data sample.

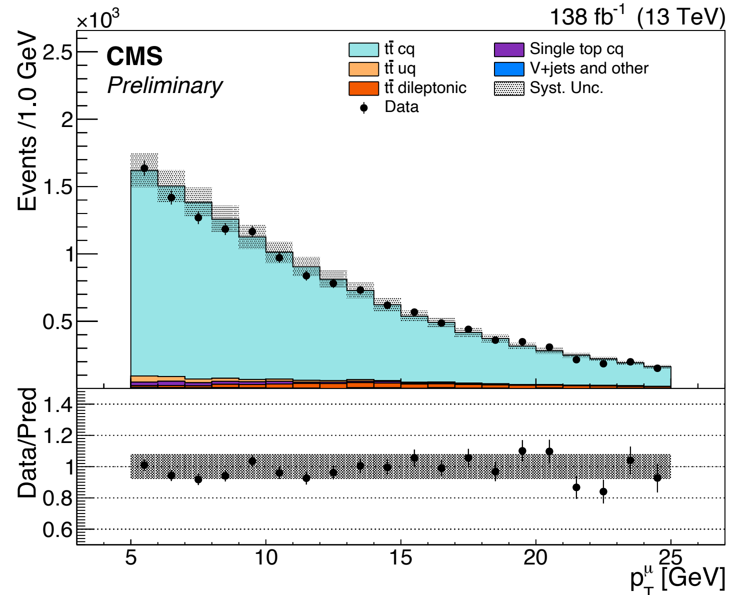

Main systematic uncertainties affecting the R_c^W

	No charm tag	Charm tag	Impact on R_c^W
Charm tagging: muon identification	—	2.7	2.6
Charm tagging: muon rate in simulation	—	2.2	2.1
Parton shower final state radiation	4.0	6.0	1.9
Total			3.9

Postfit distributions for the four event categories:

No charm-tagged, muons	No charm-tagged, electrons
Charm-tagged, muons	Charm-tagged, electrons

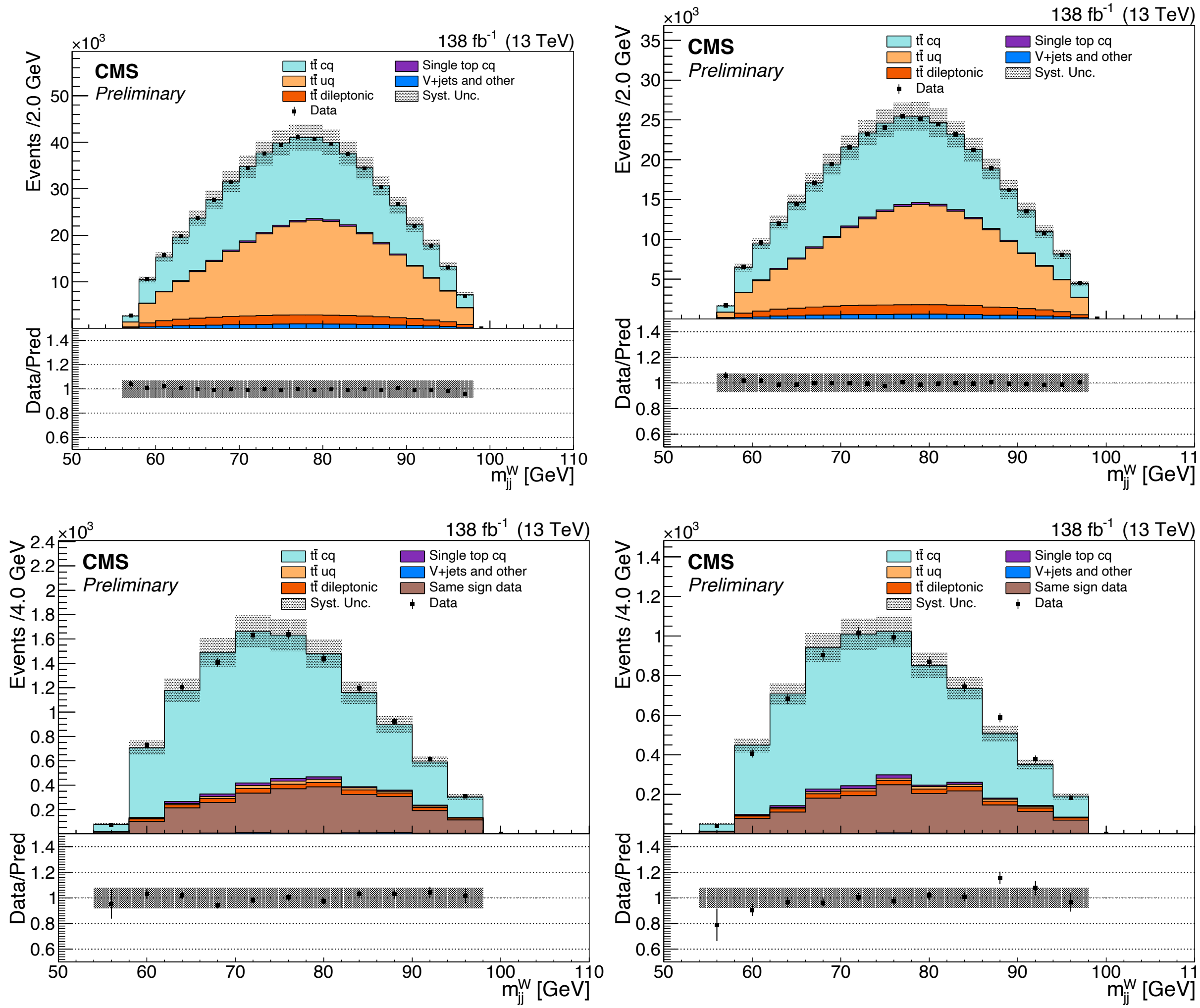

$$R_c^W = \frac{\mathcal{B}(W \to cq)}{\mathcal{B}(W \to uq) + \mathcal{B}(W \to cq)}$$

$$R_c^W = \frac{|V_{cd}|^2 + |V_{cs}|^2 + |V_{cb}|^2}{|V_{ud}|^2 + |V_{us}|^2 + |V_{ub}|^2 + |V_{cd}|^2 + |V_{cs}|^2 + |V_{cb}|^2}$$

$$R_c^W = 0.489 \pm 0.005\ (stat) \pm 0.019\ (syst) = 0.489 \pm 0.020$$

$$|V_{cs}| = 0.959 \pm 0.021$$

The sum of squared elements in the first two rows of the CKM matrix: $\Sigma = 1.984 \pm 0.021$

World-average uncertainty reduced by a factor of 2.

Precision measurement of the Z invisible width at 13 TeV

- Goal: turns generic jets+MET dark matter search on its head to make precise measurement of Z invisible width.
- Z invisible width extracted from ratio of measured cross sections of Z(vv)+jets to Z($\ell\ell$)+jets.

$$\Gamma(Z \to \nu\bar{\nu}) = \frac{\sigma(Z+\text{jets})\mathcal{B}(Z \to \nu\bar{\nu})}{\sigma(Z+\text{jets})\mathcal{B}(Z \to \ell\ell)}\Gamma(Z \to \ell\ell)$$

- Using 36.3 fb-1 of 13 TeV data
  - Jets+MET topology to select Z->vv events
  - μμ+jets and ee+jets to select Z->$\ell\ell$ events
  - μv+jets, ev+jets and τ_h v+jets for W+jets

- Backgrounds:
  - W+jets events, estimated using data driven approach and ℓ+jets control regions.
  - QCD background is estimated using data driven.
  - Contribution from γ*—>$\ell\ell$ and interference between γ*—>$\ell\ell$ and Z->$\ell\ell$ is evaluated.

Precision measurement of the Z invisible width at 13 TeV

- Invisible width extracted from simultaneous likelihood fit to the jets+MET, $\ell\ell$+jets, ℓ+jets regions
- The transfer factor estimating the W+jets background is implemented as a global unconstrained parameter scaling the W+jets process in jets+MET and ℓ+jets.

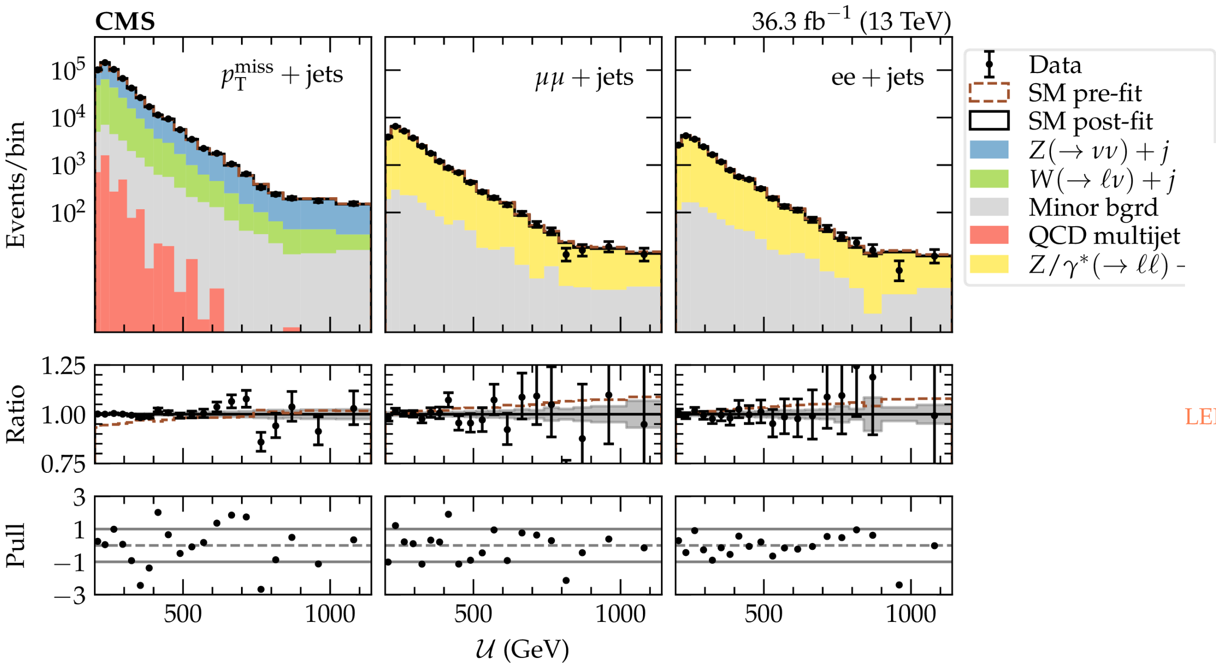

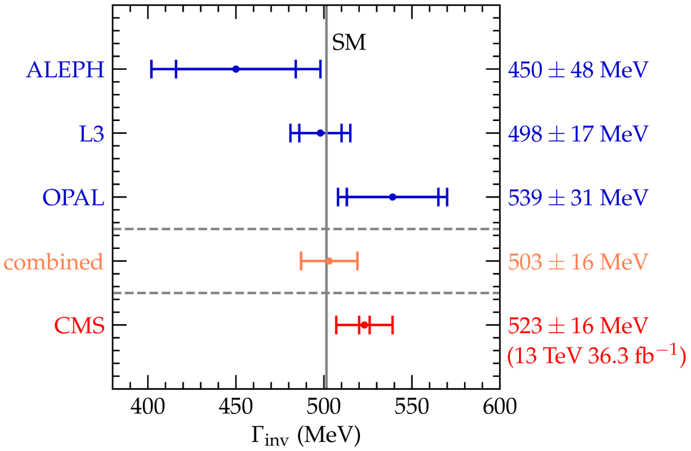

$$\Gamma_{inv} = 523 \pm 3\,(\text{stat}) \pm 16\,(\text{syst})\,\text{MeV}$$

- First direct measurement of invisible Z width at CMS.
- Precision competitive with LEP direct measurement.

Multi-differential Z+jets cross sections at 13 TeV

- Z+jets provides a sensitive evaluation of the accuracy of QCD modeling
- Using 35.9 fb-1 data to measure the differential cross section:
  - Double differential of Z pT and |*y*|
  - Jet multiplicity up to 8 jets
  - Transverse momentum and rapidities of 5 jets
  - Double differential of leading jet pT and |*y*|
  - Angular variables…

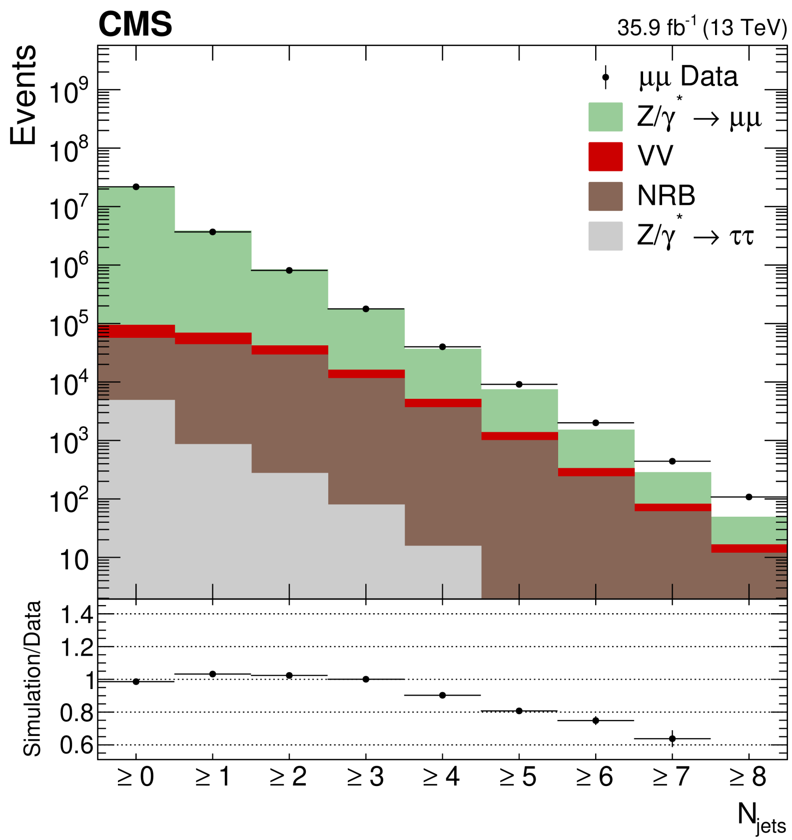

Event selections:

Opposite sign leptons with pT > 30/20GeV, |η|< 2.4
|mℓℓ −mZ |< 20GeV
Medium ID (+ 0.15 Isolation for muon)
AK4PF chs jets with pT > 30GeV, |η|< 2.4
Jets pass Loose ID and Tight WP for PU MVA
ΔR (ℓ,jets) < 0.4

Corresponding corrections and scale factors have been applied.

Multi-differential Z+jets cross sections at 13 TeV

Predictions:

- Madgraph5 NLO (Labeled NLO MG 5 aMC)
- Madgraph5 LO (Labeled LO MG 5 aMC)
- GENEVA (NNLO + NNLL resummation)

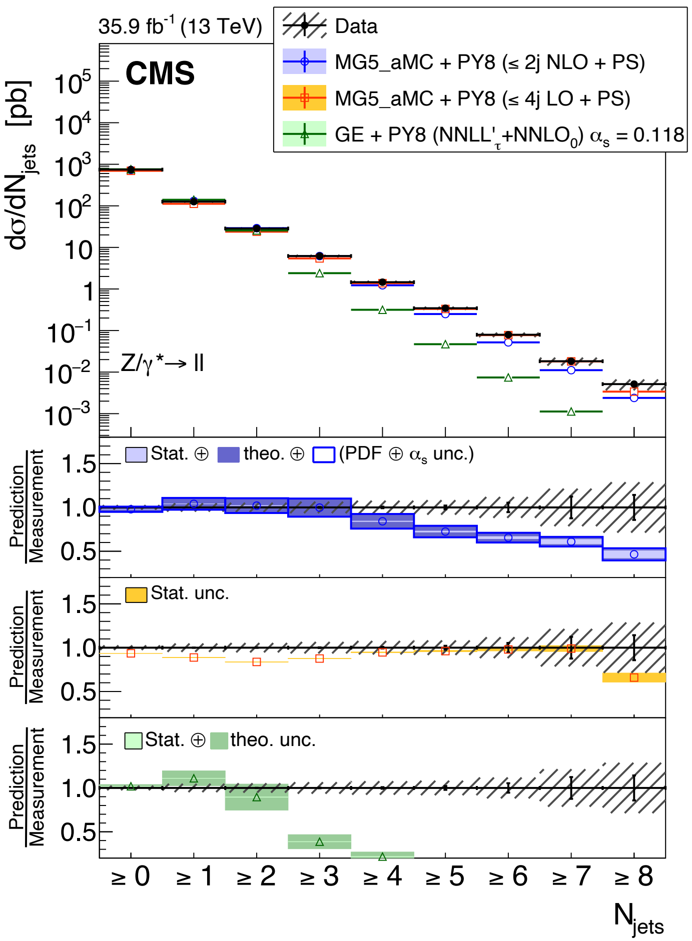

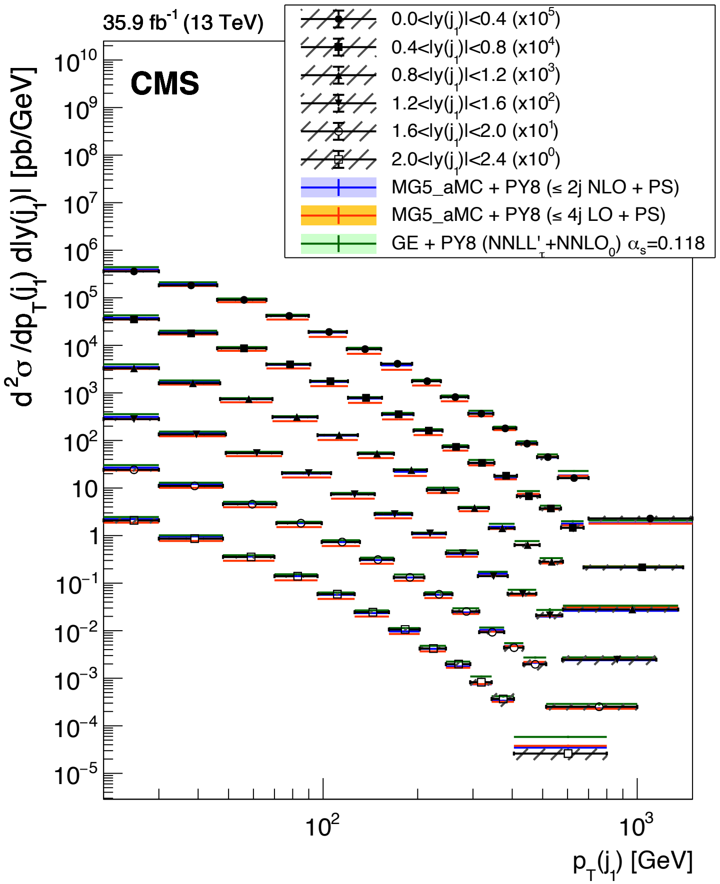

All the predictions are in agreement with data.

The NLO prediction provides a better description than LO and GENEVA for double differential cross sections.

GENEVA predicts a steeper spectrum than observed due to the lack of hard jets at ME level beyond two.

Azimuthal correlations in Z+jets at 13 TeV

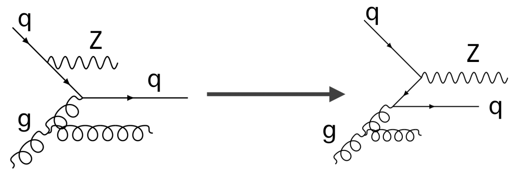

- Sensitive to higher-order corrections and soft gluon resummation.
- At small ZpT, soft-gluon resummations and nonperturbative contributions are essential.
- At high Z pT, Z+jet production is dominant with significant corrections coming from QCD processes.
- Interest in Parton Branching (PB) predictions:
  - PB method was very successful describing inclusive DY pT spectrum
  - Transverse Momentum Dependent parton distribution(TMD) and corresponding TMD parton shower are tied together, no extra free parameters.

Predictions:

- Madgraph5 NLO MPI
- Madgraph5 NLO noMPI
- GENEVA (NNLO + NNLL resummation)
- MCatNLO-CA3 (Z+1) NLO
- MCatNLO-CA3 (Z+2) NLO

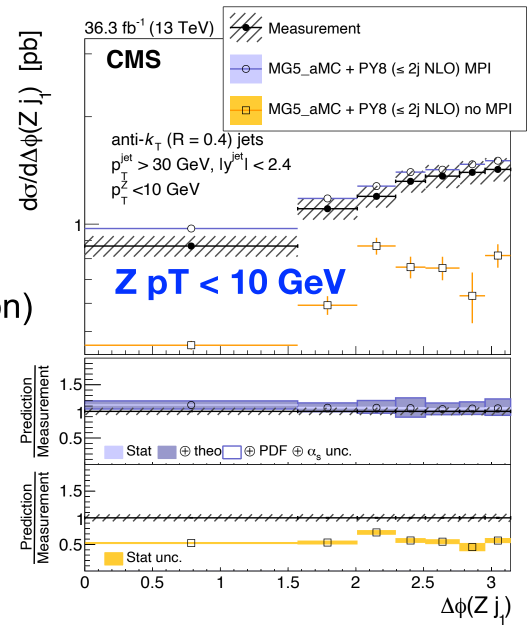

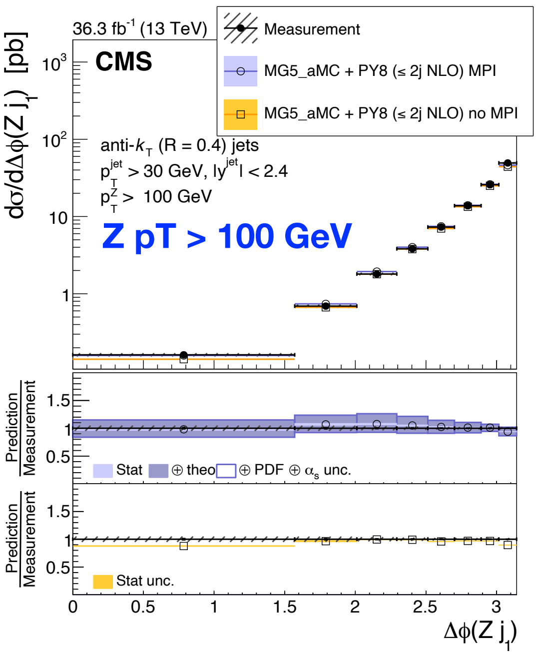

- Good agreement between data and the MG5_aMC NLO PY8 is observed.
- The contribution from MPI is about 40% for low pT(Z) region, as shown with MG5aMC no MPI

Azimuthal correlations in Z+jets at 13 TeV

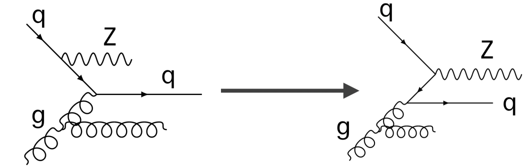

SMP-21-003

Predictions:

- Madgraph5 NLO MPI
- Madgraph5 NLO noMPI
- GENEVA (NNLO + NNLL resummation)
- MCatNLO-CA3 (Z+1) NLO
- MCatNLO-CA3 (Z+2) NLO

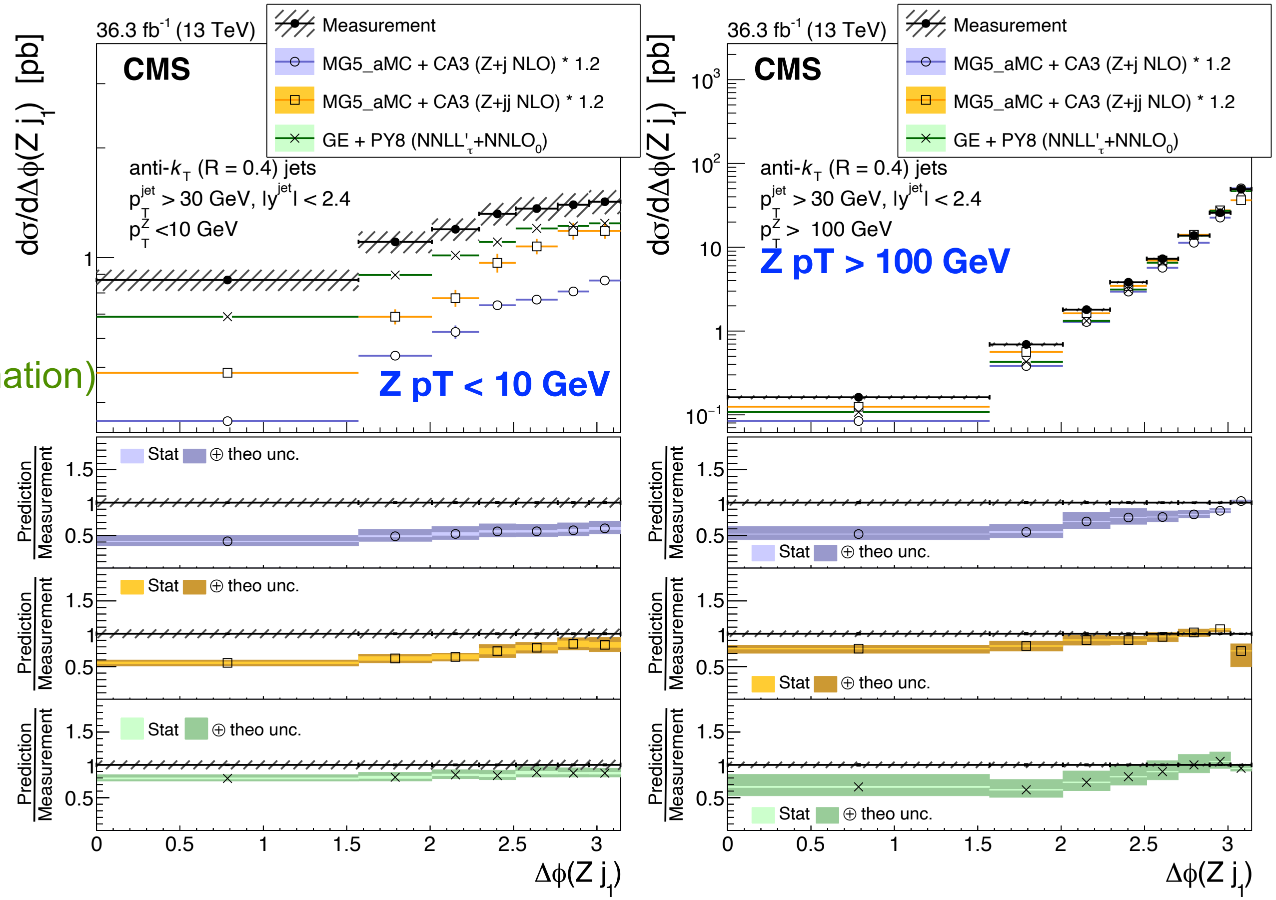

- The contribution from higher order matrix elements become important as seen from the comparison with MG5aMC + CA3 (Z+2) NLO.
- One could see the missing MPI contribution in MG5aMC+CA3 (Z+1) NLO predict, when compared to GENEVA NNLO including MPI at low pT (Z).

Summary

- Wide range physics results
  - The most precise measurement to date of the W boson hadronic decay branching fraction ratio R_c^W, and the world-average uncertainty is reduced by a factor of 2.
  - First direct measurement of invisible Z width at a hadron collider.
  - Multi-differential Drell-Yan production cross section measurements
  - NLO modelling doing well with Z/γ+jets
  - At low Z pT, the jet production is the dominant process for Z+jets process, and the Z boson could be seen as a higher order EW correction.

More results will come in the near future.

Thanks a lot for your attention!

Thank you

Measurement of B(W->cq)/B(W->qq') NEW

- Main systematic uncertainties affecting the R_c^W

	No charm tag	Charm tag	Impact on R_c^W
Charm tagging: muon identification	—	2.7	2.6
Charm tagging: muon rate in simulation	—	2.2	2.1
Parton shower final state radiation	4.0	6.0	1.9
Jet energy scale	4.0	4.0	0.6
SS data statistical uncertainty	—	1.6	0.5
Charm fragmentation modeling	—	0.4	0.3
Jet energy resolution	1.0	1.0	0.3
b tagging	2.5	2.5	0.2
MC background normalization	5.0	5.0	0.1
Integrated luminosity	1.6	1.6	0.1
Total			3.9

Introduction

- V+jets provides a sensitive evaluation of the accuracy of QCD modeling
  - Important for modeling the production mechanism involved in the Higgs boson and new physics searches.
- This process is a standard candle at LHC:
  - High cross section
  - Almost background free
  - clean signature
- It is a dominant background in many SM processes, such as Higgs production, $t\bar{t}$ production and for searches beyond SM.

Precision measurement of the Z invisible width at 13 TeV

Systematic uncertainties:

Source of systematic uncertainty	Uncertainty (%)
Muon identification efficiency (syst.)	2.1
Jet energy scale	1.8–1.9
Electron identification efficiency (syst.)	1.6
Electron identification efficiency (stat.)	1.0
Pileup	0.9–1.0
Electron trigger efficiency	0.7
τ_h veto efficiency	0.6–0.7
$p_{\mathrm{T}}^{\mathrm{miss}}$ trigger efficiency (jets plus $p_{\mathrm{T}}^{\mathrm{miss}}$ region)	0.7
$p_{\mathrm{T}}^{\mathrm{miss}}$ trigger efficiency ($\mathrm{Z}/\gamma^* \to \mu\mu$ region)	0.6
Boson p_{T} dependence of QCD corrections	0.5
Jet energy resolution	0.3–0.5
$p_{\mathrm{T}}^{\mathrm{miss}}$ trigger efficiency (μ+jets region)	0.4
Muon identification efficiency (stat.)	0.3
Electron reconstruction efficiency (syst.)	0.3
Boson p_{T} dependence of EW corrections	0.3
PDFs	0.2
Renormalization/factorization scale	0.2
Electron reconstruction efficiency (stat.)	0.2
Overall	3.2

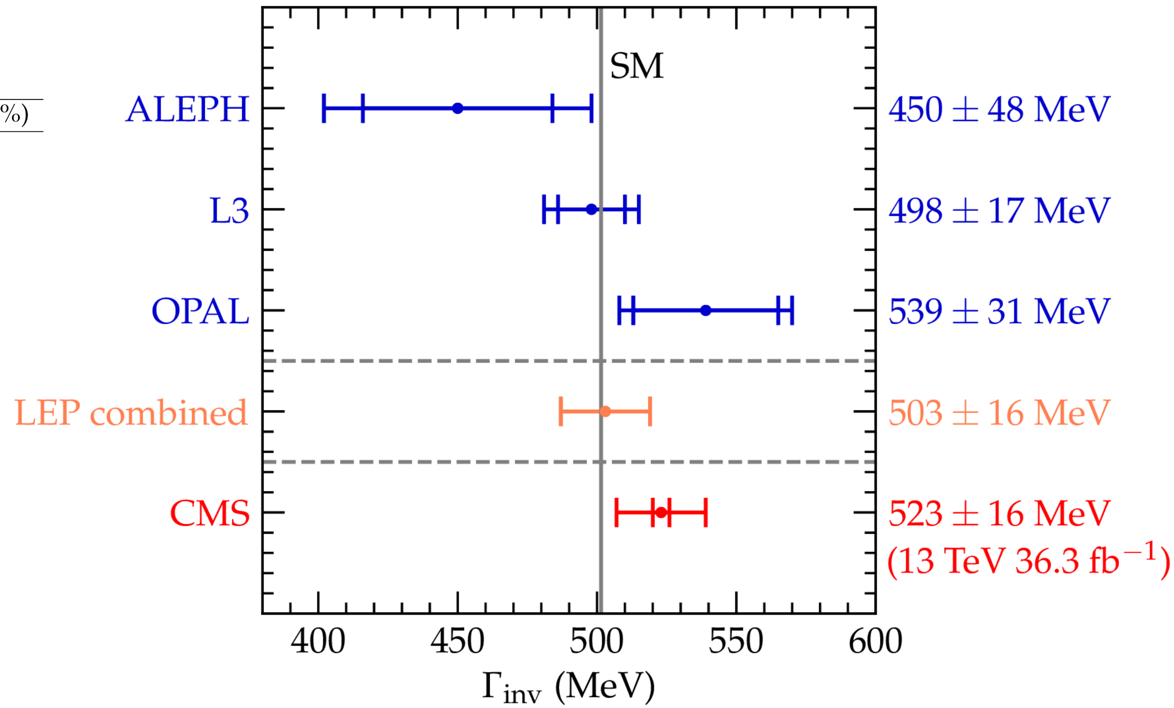

$$\Gamma_{\mathrm{inv}} = 523 \pm 3\,(\mathrm{stat}) \pm 16\,(\mathrm{syst})\,\mathrm{MeV}$$

- First direct measurement of invisible Z width at CMS
- Precision competitive with LEP direct measurement
- Most precise single direct measurement

Precision measurement of the Z invisible width at 13 TeV

Baseline

MET filters
$p_T^{miss} > 200$ GeV
$|p_{T,PF}^{miss} - p_{T,Calo.}^{miss}| / p_T^{miss} < 0.5$
Lead jet $p_T > 200$ GeV and $|\eta| < 2.4$ and $0.1 <$ Ch. Had. EF < 0.95
Veto jets $p_T > 40$ GeV and $|\eta| \geq 2.4$
Loose photon veto $p_T > 25$ GeV and $|\eta| < 2.5$
Medium CSVV2 b-jet veto $p_T > 40$ GeV and $|\eta| < 2.4$

Jets+MET

Baseline
Loose muon veto $p_T > 10$ GeV and $|\eta| < 2.5$
Veto electron veto $p_T > 10$ GeV and $|\eta| < 2.5$
Very loose tau veto $p_T > 20$ GeV and $|\eta| < 2.3$
$\min[\Delta\phi(j_{1,2,3,4}, p_T^{miss})] > 0.5$

Double Muon

Baseline
2 medium muons $p_T > 25$ GeV and $|\eta| < 2.4$
Veto electron veto $p_T > 10$ GeV and $|\eta| < 2.5$
Very loose tau veto $p_T > 20$ GeV and $|\eta| < 2.3$
$71 < M_{\mu\mu} < 111$ GeV
$\min[\Delta\phi(j_{1,2,3,4}, p_T^{miss})] > 0.5$

Double Electron

Baseline
2 medium electrons $p_T > 30$ GeV and $|\eta| < 2.4$
Loose muon veto $p_T > 10$ GeV and $|\eta| < 2.5$
Very loose tau veto $p_T > 20$ GeV and $|\eta| < 2.3$
$71 < M_{ee} < 111$ GeV
$\min[\Delta\phi(j_{1,2,3,4}, p_T^{miss})] > 0.5$

Single Muon

Baseline
1 medium muon $p_T > 25$ GeV and $|\eta| < 2.4$
Veto electron veto $p_T > 10$ GeV and $|\eta| < 2.5$
Very loose tau veto $p_T > 20$ GeV and $|\eta| < 2.3$
$30 \leq M_T(\mu, p_{T,PF}^{miss}) < 125$ GeV
$\min[\Delta\phi(j_{1,2,3,4}, p_T^{miss})] > 0.5$

Single Electron

Baseline
1 medium electron $p_T > 30$ GeV and $|\eta| < 2.4$
Loose muon veto $p_T > 10$ GeV and $|\eta| < 2.5$
Very loose tau veto $p_T > 20$ GeV and $|\eta| < 2.3$
$p_{T,PF}^{miss} > 100$ GeV
$30 \leq M_T(e, p_{T,PF}^{miss}) < 125$ GeV
$\min[\Delta\phi(j_{1,2,3,4}, p_T^{miss})] > 0.5$

Single Tau

Baseline
1 tight tau $p_T > 40$ GeV and $|\eta| < 2.3$
Loose muon veto $p_T > 10$ GeV and $|\eta| < 2.5$
Veto electron veto $p_T > 10$ GeV and $|\eta| < 2.5$
$\min[\Delta\phi(j_{1,2,3,4}, p_T^{miss})] > 0.5$

QCD sideband

Baseline
Loose muon veto $p_T > 10$ GeV and $|\eta| < 2.5$
Veto electron veto $p_T > 10$ GeV and $|\eta| < 2.5$
Very loose tau veto $p_T > 20$ GeV and $|\eta| < 2.3$
$\min[\Delta\phi(j_{1,2,3,4}, p_T^{miss})] \leq 0.5$

5

Precision measurement of the Z invisible width at 13 TeV

Table 1: Relative uncertainties (in %) on the final measurement from different sources.

Source of systematic uncertainty	Uncertainty (%)
Muon identification efficiency (syst.)	2.1
Jet energy scale	1.8–1.9
Electron identification efficiency (syst.)	1.6
Electron identification efficiency (stat.)	1.0
Pileup	0.9–1.0
Electron trigger efficiency	0.7
τ_h veto efficiency	0.6–0.7
p_T^{miss} trigger efficiency (jets plus p_T^{miss} region)	0.7
p_T^{miss} trigger efficiency ($Z/\gamma^* \to \mu\mu$ region)	0.6
Boson p_T dependence of QCD corrections	0.5
Jet energy resolution	0.3–0.5
p_T^{miss} trigger efficiency (μ+jets region)	0.4
Muon identification efficiency (stat.)	0.3
Electron reconstruction efficiency (syst.)	0.3
Boson p_T dependence of EW corrections	0.3
PDFs	0.2
Renormalization/factorization scale	0.2
Electron reconstruction efficiency (stat.)	0.2
Overall	3.2

Precision measurement of the Z invisible width at 13 TeV

- Invisible width extracted from simultaneous likelihood fit to the jets+MET, $\ell\ell$+jets, ℓ+jets regions

$$\mathcal{L}(n_j, n_\ell, n_{\ell\ell} | r, r_Z, r_W, \boldsymbol{\theta}) =$$
$$\text{Poisson}\left(n_j \,\middle|\, r \cdot r_Z \cdot s_{Z,j}(\boldsymbol{\theta}) + r_W \cdot b_{j,W}(\boldsymbol{\theta}) + b_{\text{bkg.},j}(\boldsymbol{\theta})\right)$$ Jets+MET
$$\text{Poisson}\left(n_\ell \,\middle|\, r_W \cdot b_{\ell,W}(\boldsymbol{\theta}) + b_{\text{bkg.},\ell}(\boldsymbol{\theta})\right)$$ Single lepton
$$\text{Poisson}\left(n_{\ell\ell} \,\middle|\, r_Z \cdot s_{Z,\ell\ell}(\boldsymbol{\theta}) + \sqrt{r_Z} \cdot s_{\text{int.},\ell\ell} + s_{\gamma^*,\ell\ell}(\boldsymbol{\theta}) + b_{\text{bkg.},\ell\ell}(\boldsymbol{\theta})\right)$$ Double lepton
$$\cdot\, p(\tilde{\boldsymbol{\theta}}, \boldsymbol{\theta})$$

$$\Gamma(Z \to \nu\bar{\nu}) = \frac{\sigma(Z+\text{jets}) \cdot B(Z \to \nu\bar{\nu})}{\sigma(Z+\text{jets}) \cdot B(Z \to \ell\ell)} \Gamma(Z \to \ell\ell)$$
$$= \frac{\varepsilon_{\ell\ell}\mathcal{A}_{\ell\ell}}{\varepsilon_{\nu\nu}\mathcal{A}_{\nu\nu}} \frac{r \cdot r_Z \cdot s_{Z,j}(\boldsymbol{\theta})}{r_Z \cdot s_{Z,\ell\ell}(\boldsymbol{\theta})} \Gamma(Z \to \ell\ell)$$
$$= r \frac{\varepsilon_{\ell\ell}\mathcal{A}_{\ell\ell}}{\varepsilon_{\nu\nu}\mathcal{A}_{\nu\nu}} \frac{s_{Z,j}(\boldsymbol{\theta})}{s_{Z,\ell\ell}(\boldsymbol{\theta})} \Gamma(Z \to \ell\ell).$$

$$\Gamma_{\text{MC}}(Z \to \nu\bar{\nu}) = \frac{\varepsilon_{\ell\ell}\mathcal{A}_{\ell\ell}}{\varepsilon_{\nu\nu}\mathcal{A}_{\nu\nu}} \frac{s_{Z,j}(\boldsymbol{\theta})}{s_{Z,\ell\ell}(\boldsymbol{\theta})} \Gamma_{\text{MC}}(Z \to \ell\ell)$$

$$r_{\text{inv}} \equiv r = \frac{\Gamma(Z \to \text{inv})}{\Gamma_{\text{MC}}(Z \to \text{inv})}$$

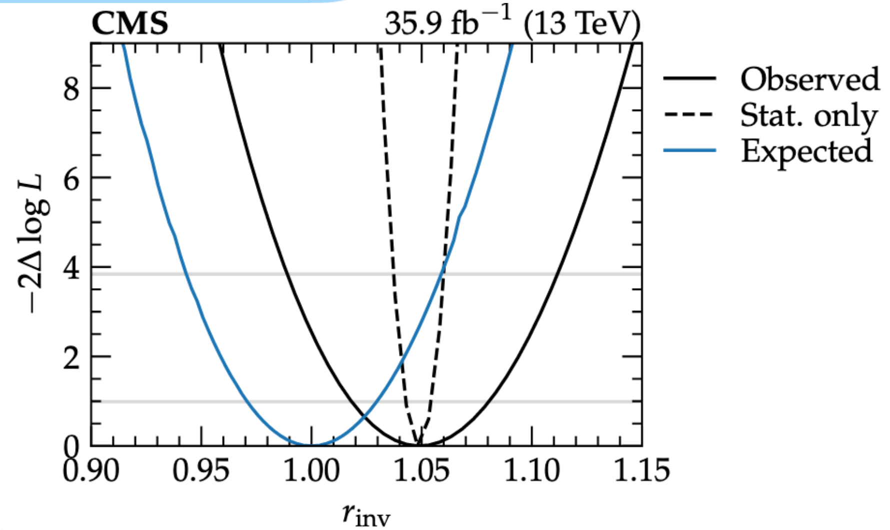

$$r_{\text{inv}} = 1.052 \pm 0.006(\text{stat})^{+0.032}_{-0.031}(\text{syst})$$

Using input Z width of 510 MeV:

$$\Gamma_{\text{inv}} = 523 \pm 3\,(\text{stat}) \pm 16\,(\text{syst})\,\text{MeV}$$

Multi-differential Z+jets cross sections at 13 TeV

SMP-19-009

- Clean event selection with percent level background and well understood recoil object with the Z boson

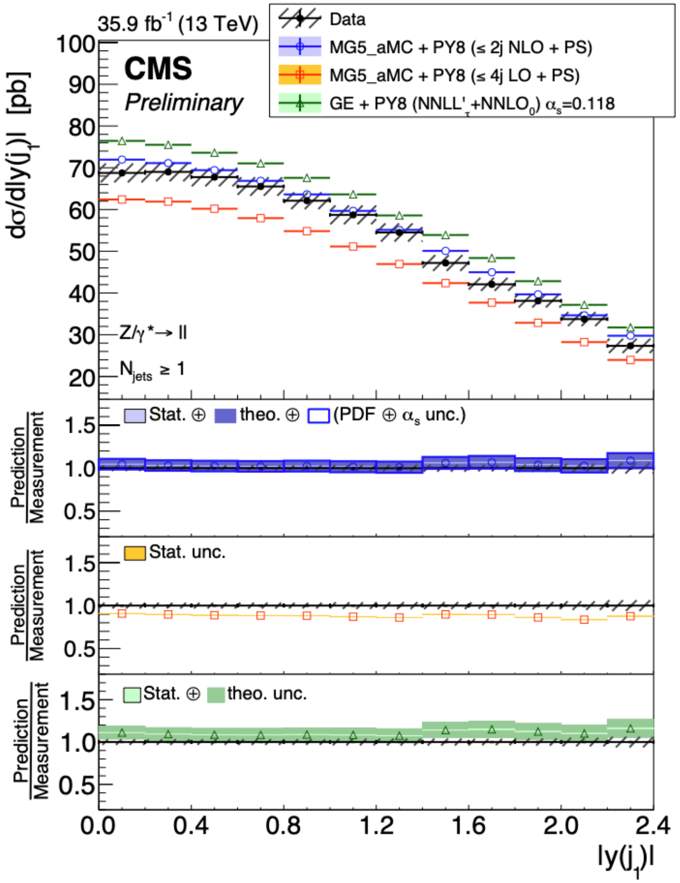

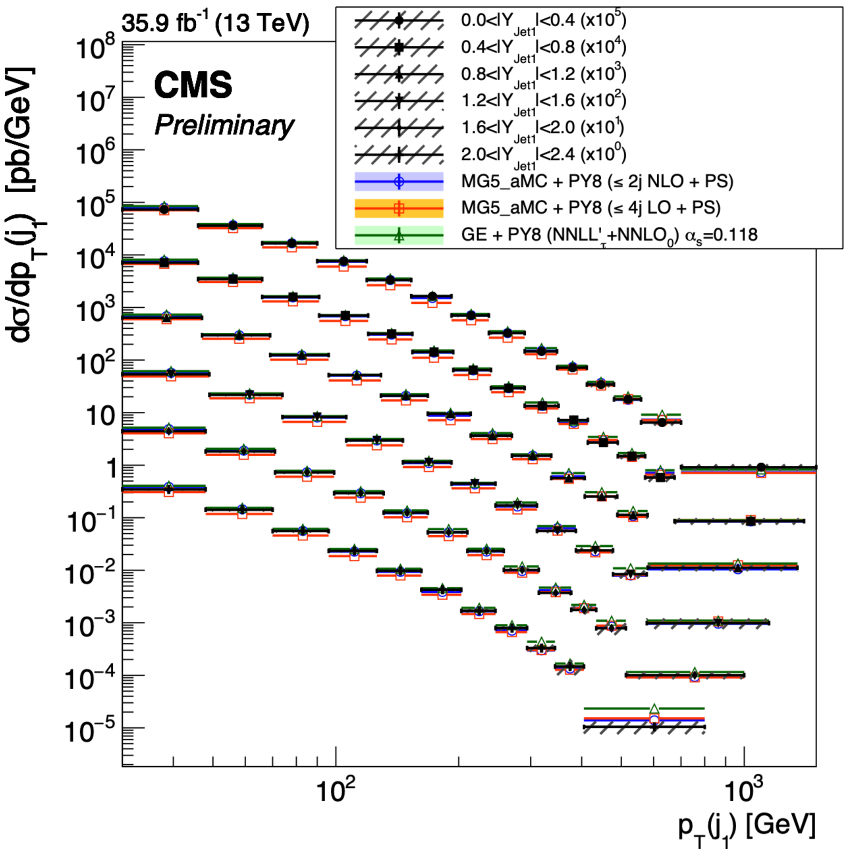

Multi-differential Z+jets cross sections at 13 TeV

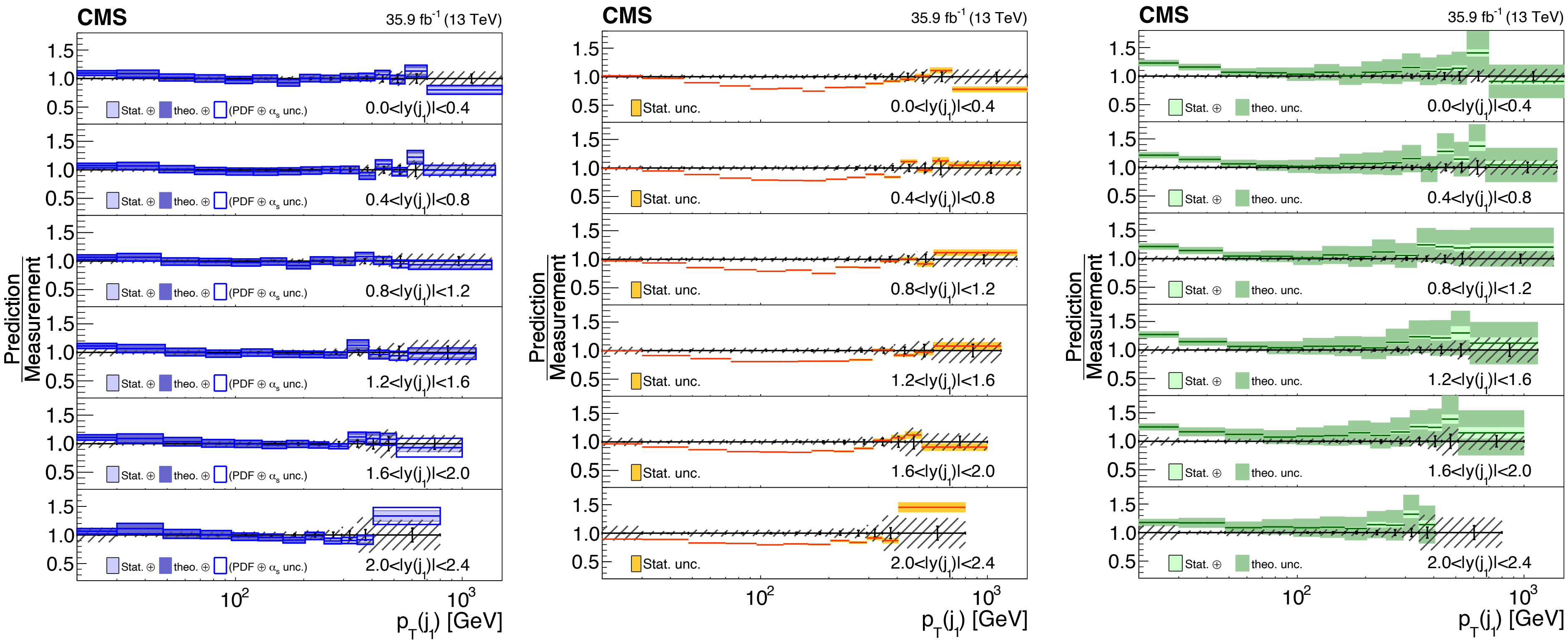

- All the predictions are in agreement with data.
- The NLO prediction provides a better description than LO and GENEVA for double differential cross sections.

Results-dPhi(jet1, jet2)

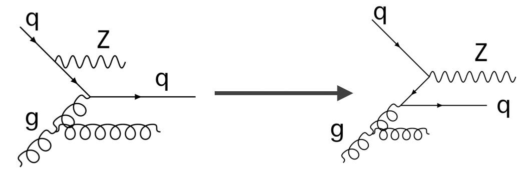

Z pT < 10 GeV

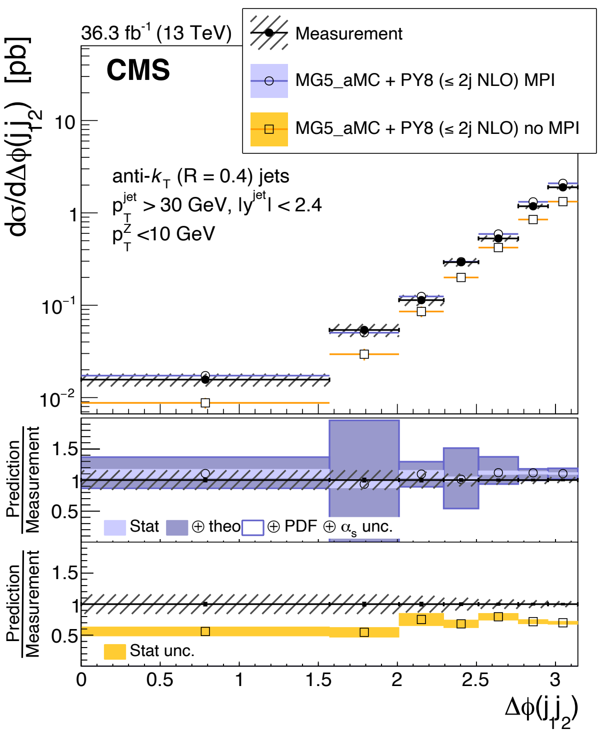

Z pT (30, 50) GeV

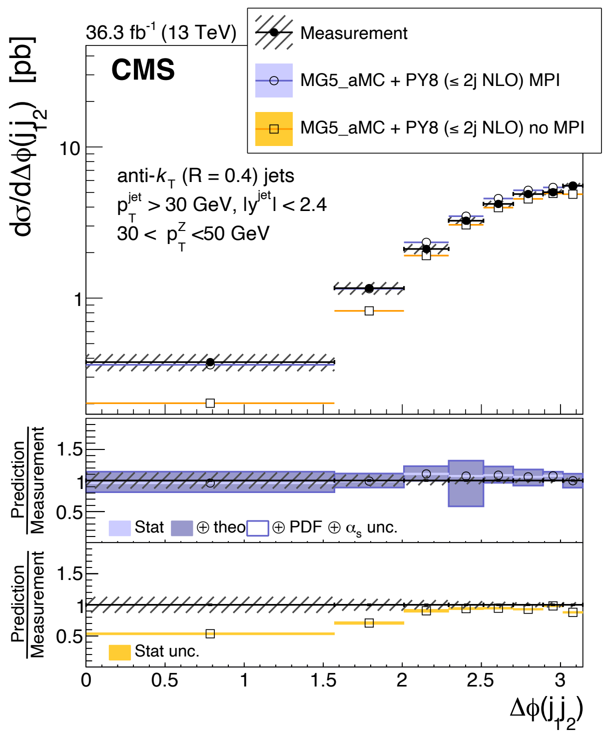

Z pT > 100 GeV

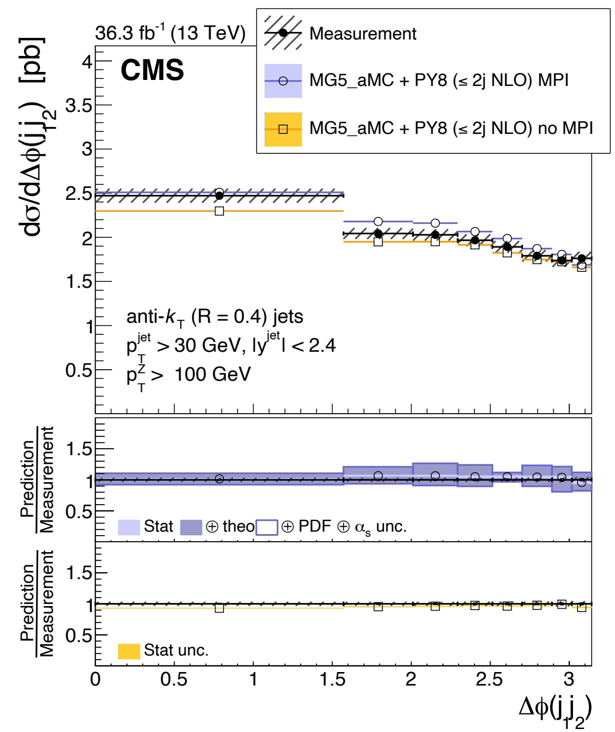

- A strong correlation between the two leading jets is observed at small Z pT, indicating that at low Z pT the process is dominated by jet production and the Z boson is radiated as a higher order EW correction.
- At large Z pT the process is dominated by Z+jet production, with higher order QCD corrections in form of additional jets.
- The contribution from MPI is significant especially at small Z pT, and small dPhi(j1,j2).

Results-dPhi(jet1, jet2)

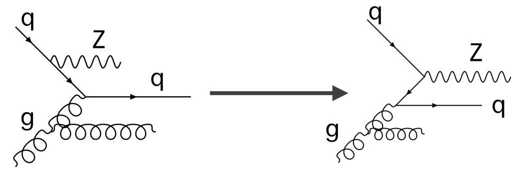

Z pT < 10 GeV

Z pT (30, 50) GeV

Z pT > 100 GeV

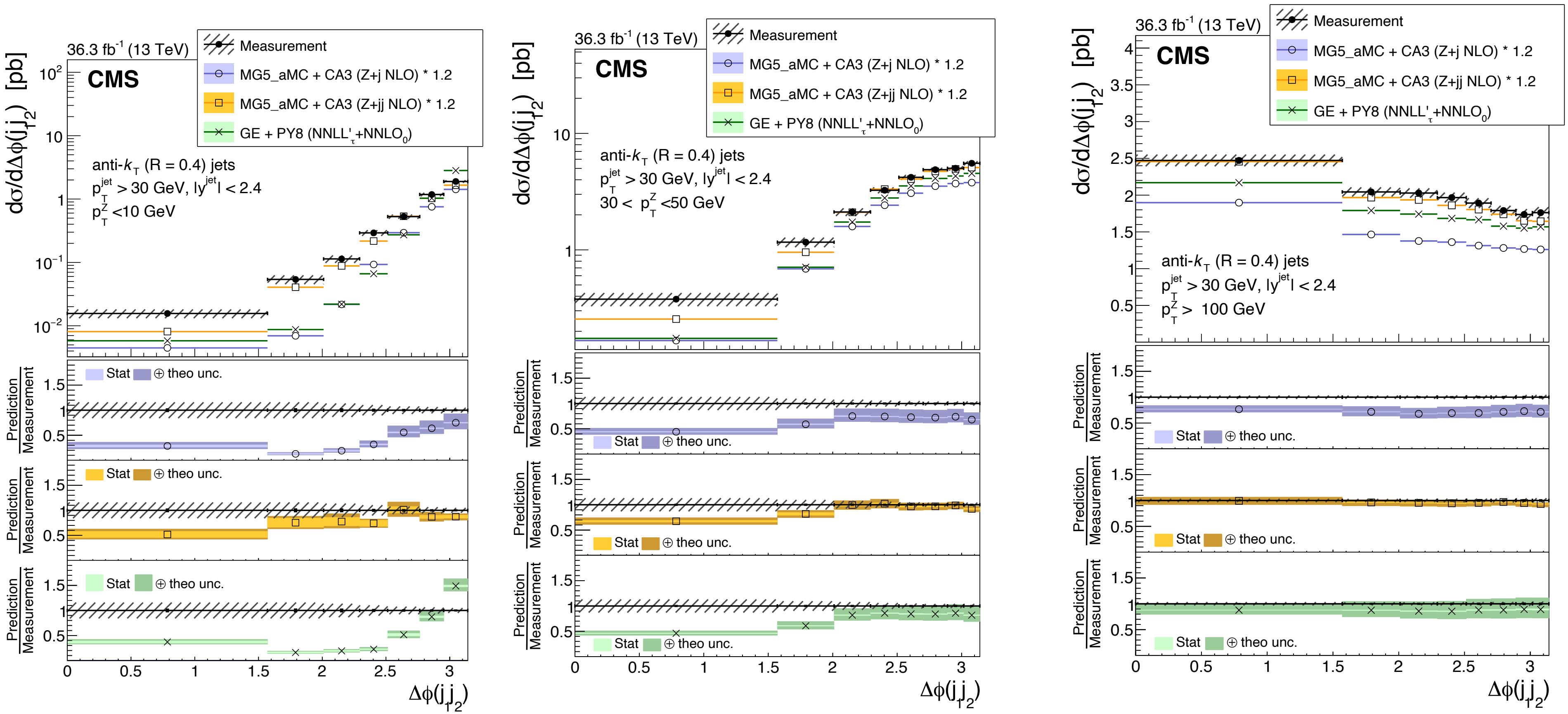

- At larger dPhi (j1, j2) region, the measurement is reasonably well described by MG5aMC + CA3 (Z+2) NLO , while it falls at lower dPhi region presumably because of missing MPI contribution.
- The GENEVA NNLO prediction is below the measurement, and it is similar to MG5aMC+CA3 (Z+1) NLO predict prediction.

Azimuthal correlations in Z+jets at 13 TeV

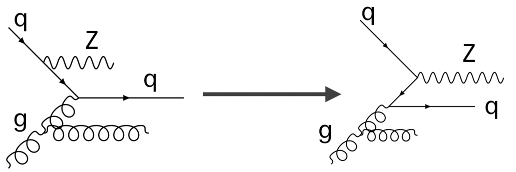

SMP-21-003

Predictions:

- Madgraph5 NLO MPI
- Madgraph5 NLO noMPI
- GENEVA (NNLO + NNLL resum
- MCatNLO-CA3 (Z+1) NLO
- MCatNLO-CA3 (Z+2) NLO

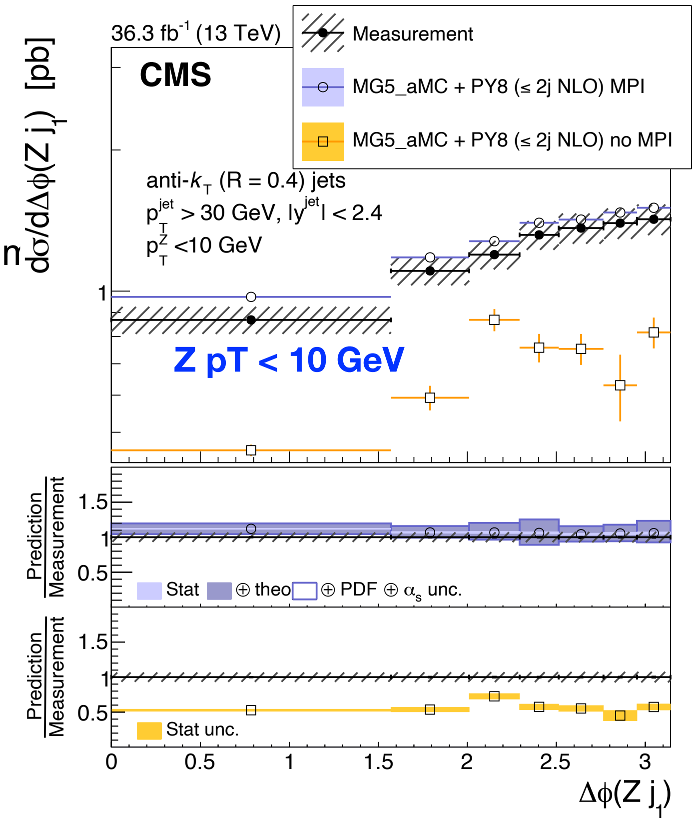

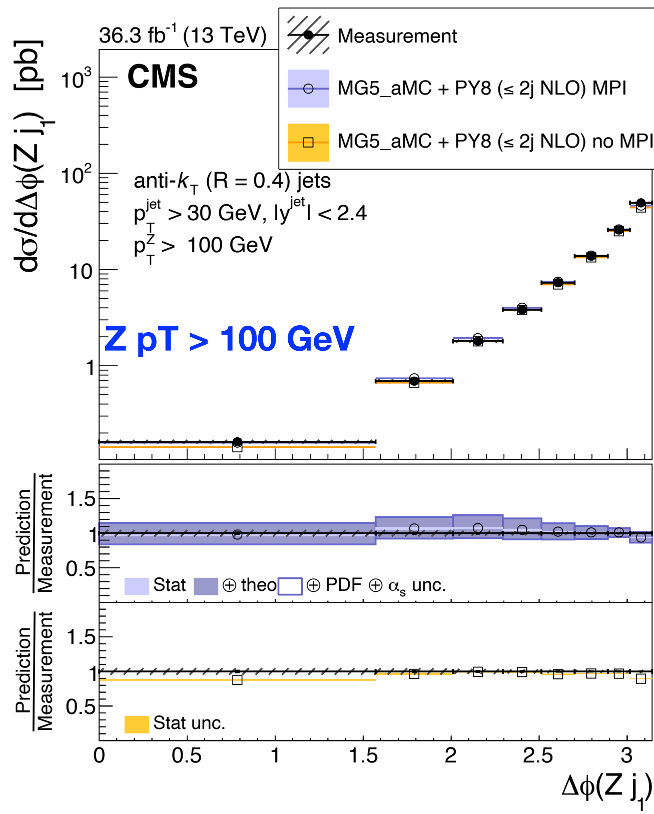

- Good agreement between data and the MG5_aMC NLO PY8 is observed.
- In the low pT(Z) region, the Z boson is only weakly correlated with the leading jet, and the distribution is flat.
- In the large pT(Z) region, Z boson is highly correlated with the leading jet, and peaks in the back-to-back region.
- The contribution from MPI is about 40% for low pT(Z) region, as shown with MG5aMC no MPI